Deconstructing Spatiotemporal Chaos Using Local Symbolic Dynamics

Shawn D. Pethel and Ned J. Corron
AMSRD-AMR-WS-ST, U.S. Army RDECOM, Redstone Arsenal, Alabama 35898, USA

Erik Bollt
Department of Math and Computer Science, Clarkson University, Potsdam, New York 13699-5805, USA
(Received 30 September 2006; published 19 November 2007)

We find that the global symbolic dynamics of a diffusively coupled map lattice is well approximated by a very small local model for weak to moderate coupling strengths. A local symbolic model is a truncation of the full symbolic model to one that considers only a single element and a few neighbors. Using interval analysis, we give rigorous results for a range of coupling strengths and different local model widths. Examples are presented of extracting a local symbolic model from data and of controlling spatiotemporal chaos.

DOI: 10.1103/PhysRevLett.99.214101 PACS numbers: 05.45.Jn, 05.45.Ra

In this Letter, we approximate the global symbolic dynamics of a diffusively coupled map lattice (CML) with a local model consisting of a relatively small number of symbols. Coupled map lattices [1] are popular models of spatiotemporal chaos, and their description via symbolic dynamics provides a complete basis for understanding them. Indeed, the topology of unimodal maps has been completely elucidated in terms of 2-symbol alphabets [2], and recently it has been conjectured that these results extend simply to the CML case [3]. Nevertheless, one still has to contend with the high dimensionality of lattices. While a single logistic map is fully described by 2 symbols, an N-element lattice requires an alphabet of 2^N symbols. In the case of diffusive coupling, however, we find that the symbolic dynamics at a particular site is largely determined by a local neighborhood, at least for some range of coupling strengths. Previously, it has been shown that the symbol statistics at a single site can indicate degrees of global synchronization [4]. Here we propose using symbolic information from a small neighborhood to reconstruct the dynamics of the entire lattice. In what follows we use interval analysis to quantify this idea and to show that the global symbolic dynamics can be well approximated by a compact local model for weak to moderate coupling strengths.

We consider a map lattice with N sites labeled $i = 1, \ldots, N$. Each site is described by a state x_t^i in the interval I^i and a unimodal local dynamic f_i: $I^i \to I^i$. Denote by F the product function of f_i onto each site, and by A an $N \times N$ coupling matrix, then the map lattice can be written as $\mathbf{x}_{t+1} = H(\mathbf{x}_t)$, where $H = A \circ F$. Models of this type have been extensively studied with regard to turbulence and pattern formation [5]. Here we introduce an alternate formulation in terms of local symbolic dynamics.

As reported previously [3], it is conjectured that for nonsingular A a homeomorphism exists between the spatiotemporal sequence $\{x_t^i: i = 1, \ldots, N, t \geq 0\}$ and the equivalently sized set of binary symbols s_t^i defined by

$$s_t^i = \begin{cases} 0 & \text{if } x_t^i \in I_0^i, \\ 1 & \text{if } x_t^i \in I_1^i, \end{cases} \tag{1}$$

where I_0^i and I_1^i are the two subintervals over which the unimodal map f_i is monotonic. Figures 1(a) and 1(b) illustrate this mapping for a CML of logistic maps. The particular state x_t^i is homeomorphic to s_t^i plus the set of all

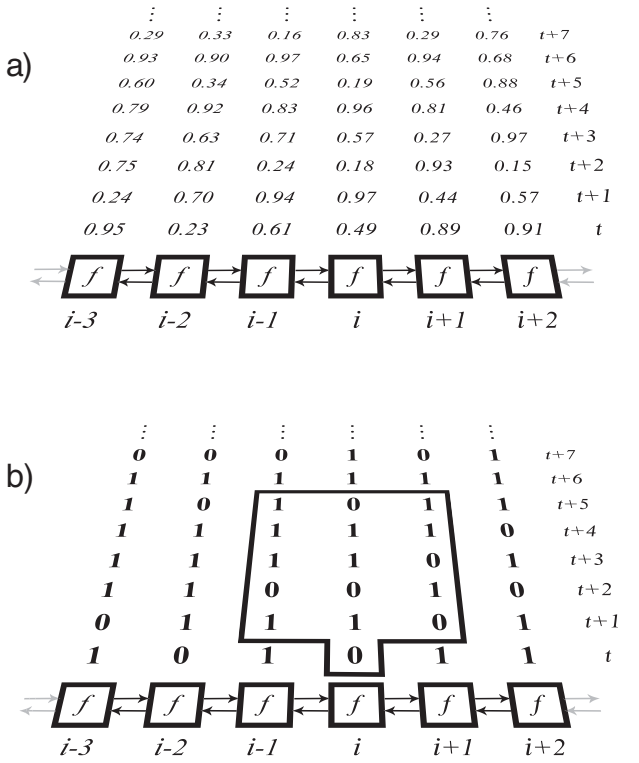

FIG. 1. A time-space segment of a 1D CML of logistic maps. (a) Real valued CML states (shown with 2 digits of precision), (b) the equivalent symbolic representation using $I_0 = [0, 0.5)$ and $I_1 = [0.5, 1]$. A $m = 3$, $n = 5$ local symbolic representation of x_t^i is shown outlined.

future symbols. This relationship can be understood in the following way. Consider that the symbol vector $\mathbf{s}_{t+n}$ indicates which subinterval the components of $\mathbf{x}_{t+n}$ lie in. Provided one knows which preimage to use, $\mathbf{x}_{t+n-1}$ can be estimated by applying H^{-1} onto this vector of subintervals. The symbol vector $\mathbf{s}_{t+n-1}$ resolves the preimage ambiguity because the branches of f_i^{-1} lie on unique monotonic segments labeled by $\{0, 1\}$. Repeat this process until an estimate of $\mathbf{x}_t$ is reached. At the last step only the symbol s_t^i is required to estimate x_t^i. Because the inverse of a chaotic map is (on average) contracting, the estimate converges to x_t^i as $n \to \infty$.

Let $P_{\mathbf{s}_t}$ be the vector of subintervals containing the CML state at time t. The first n terms of the above algorithm can be expressed as

$$\{\mathbf{x}_0\}_{\mathbf{s}_0 \cdots \mathbf{s}_{n-1}} = I^N \cap H_{\mathbf{s}_0}^{-1} \circ \cdots \circ H_{\mathbf{s}_{n-2}}^{-1} P_{\mathbf{s}_{n-1}}, \\ = I^N \cap (F_{\mathbf{s}_0}^{-1} A^{-1}) \circ \cdots \circ (F_{\mathbf{s}_{n-2}}^{-1} A^{-1}) P_{\mathbf{s}_{n-1}}, \quad (2)$$

where I^N is the N dimensional domain of H and the subscript on F^{-1} specifies a particular inverse branch. The left-hand side is the set of all states that produce the sequence $\mathbf{s}_0 \cdots \mathbf{s}_{n-1}$. An empty set implies a forbidden sequence.

Exact evaluation of Eq. (2) is difficult; however, it is amenable to *interval analysis* [6]. This method utilizes interval arithmetic for the purpose of achieving rigorous bounds on the solution space. In this case, interval computations result in guaranteed, tight bounds on the components of the vector $\mathbf{x}_0$ given some symbol sequence. Tightness is a consequence of the monotonicity of $F_{\mathbf{s}}^{-1}$, and is significant because it implies that the interval approximation converges with symbol depth n at the same rate as Eq. (2).

Using interval arithmetic, the local symbolic dynamics can be investigated rigorously. We define the local symbolic representation of a CML site x_t^i to be the symbols in a neighborhood of spatial width m and temporal depth n. Because the symbols s_t^j, $j \neq i$ are irrelevant to x_t^i we are effectively left with the paddle-shaped region illustrated in Fig. 1(b). Restricting Eq. (2) to the local neighborhood requires using a full interval for each unspecified component of $P_{\mathbf{s}_{n-1}}$ and taking the union of the two preimages at each of these sites. In this way we can compute guaranteed bounds on x_t^i given only knowledge of symbols in a local neighborhood.

As mentioned earlier, we expect the local symbolic model to be suitable for diffusively coupled systems. From Eq. (2) we see that the symbols are related to the CML state via repeated applications of the inverse mapping, $H^{-1} = F^{-1} \circ A^{-1}$. In the case that the coupling matrix A is tridiagonal—i.e., the CML employs nearest neighbor coupling—the elements of A^{-1} can be found analytically [7] and shown to fall off exponentially in magnitude with increasing offset from the diagonal. A major point here is that the symbolic dynamics at site i is largely determined by a small neighborhood $m \ll N$, at least for some range of coupling strengths. Importantly, the local model requires only $mn - m + 1$ symbols and is independent of the lattice size N.

Having defined our local model approach, let us investigate its efficacy in terms of the commonly studied 1D CML written as

$$x_{t+1}^i = (1 - \epsilon) f(x_t^i) + \frac{\epsilon}{2}[f(x_t^{i-1}) + f(x_t^{i+1})], \quad (3)$$

with periodic boundaries [5]. The coupling parameter $\epsilon \in [0, 0.5]$ sets the diffusion rate. Staying with convention we use the logistic map $f(x) = 4x(1 - x)$ as the local dynamic; therefore, the symbol "0" corresponds to site values in the interval $I_0 = [0, 0.5)$ and the symbol "1" to the interval $I_1 = [0.5, 1]$. For large N, the off-diagonal terms of A^{-1} decay in magnitude as $(\epsilon/(2 - 2\epsilon))^{|\delta|}$, where δ is the offset from the diagonal [7]. The restriction of the local model to nearest neighbor symbols ($m = 3$) is tantamount to neglecting the $\delta \geq 2$ elements of A^{-1}, which, at the moderate coupling strength $\epsilon = 0.1$, are less than 1% of the diagonal terms.

We gauge the fidelity of the local symbolic model by its mean error over a test CML trajectory. The test data are symbolized and Eq. (2) is used to produce an interval estimate at each CML site x_t^i for various local model sizes and coupling strengths. We define the expected value $\tilde{x}_t^i$ to be the midpoint of this interval and compute a mean absolute error $E = \langle |x_t^i - \tilde{x}_t^i| \rangle$ over the data set. In Fig. 2 we plot E versus symbol depth n, and coupling strength ϵ for an $N = 128$ lattice of logistics maps. The test data are

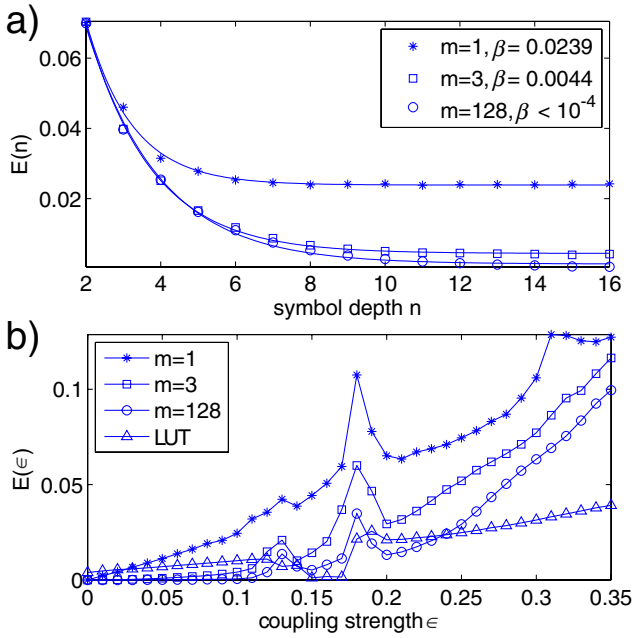

FIG. 2 (color online). Mean absolute error E for $m = 1$, $m = 3$, and the global symbolic model ($m = 128$) of a logistic CML of 128 elements. (a) E versus symbol depth n for $\epsilon = 0.1$. β is the extrapolated value of $E(n)$ for $n \to \infty$; (b) E versus coupling strength ϵ for $n = 16$.

10^4 iterations of the CML starting from a random initial condition. These errors should be compared to the $[0, 1]$ range of the dynamics at each site.

As seen in Fig. 2(a), the fidelity of the local model improves smoothly with increasing n. The error is shown fitted to the function, $E(n) \approx \alpha e^{-\lambda n} + \beta$, for $\epsilon = 0.1$ and for the cases of no neighboring symbolic information ($m = 1$), nearest neighbors only ($m = 3$), and for the global symbolic model ($m = 128$). The value β is the extrapolated limit of $E(n)$ for $n \to \infty$. The $m = 3$ local model performs well compared to the global model; for $n \leq 6$ there is very little difference in fidelity. We note that at $n = 6$, the local model requires only 16 symbols ($3 \times 6 - 2$) to achieve an error of approximately 1% of the $[0, 1]$ dynamic range at each site. After $n = 10$, the $m = 3$ model hits an error floor ($\beta = 0.0044$), whereas the global model asymptotes to zero error.

In Fig. 2(b), n is fixed at 16 and the error is shown versus coupling strength. In the region of weak to moderate coupling strength ($\epsilon \leq 0.11$) the error is small and there is good agreement between the $m = 3$ local model and the global model. For strong coupling ($\epsilon \geq 0.2$), the error grows steeply for the global model, and therefore for the local models as well. The error in this case is not so much due to the local symbol approximation, but to slow convergence of Eq. (2) with respect to n. The region $\epsilon \in [0.12, 0.18]$ contains nonchaotic states, for which our definition of $E(n)$ is not intended; we include this region only for completeness.

Given that there is merit to the local model approach, we now formalize the theory. Define a local symbolic model as the set $\mathcal{S}^i$ of at most 2^{mn-m+1} elements representing all truncated symbol patterns that are allowed by the dynamics at site i. By "pattern" we mean a particular arrangement of symbols within the $m \times n$ paddle-shaped window [Fig. 1(b)]. A *global* symbolic state $\mathbf{S}_{k_1 \ldots k_N} = \mathcal{S}^1_{k_1} \mathcal{S}^2_{k_2} \cdots \mathcal{S}^N_{k_N}$ is an overlapping concatenation of local symbolic states, where k_i indexes an element of $\mathcal{S}^i$. An overlapping concatenation is possible between two local symbolic states only if overlapping symbols match. The approximated global symbolic dynamics can now be defined as the set $\{\mathbf{S}_{k_1 \ldots k_N}\}$ of all overlapping concatenations of local symbolic states. Obviously, any incompatibilities that occur outside the spatial and temporal boundaries of the local model are not accounted for in this approximation. The set $\{\mathbf{S}_{k_1 \ldots k_N}\}$ is therefore a superset of the actual global symbolic model.

Local models are a compact means of describing the global symbolic dynamics of the CML. If we define the complexity of a set to be the growth rate of its cardinality, then the maximum complexity of the entire collection of local models is $\mathcal{O}(N 2^{mn-m+1})$. This extreme assumes that a different local model must be used at each site. Importantly, the complexity of local model approach scales at worst linearly with N, whereas the exact symbolic description scales as 2^{Nn}.

There are two major features of the local symbolic model that we emphasize and elaborate on here. The first is that local models can be small enough to compile from data and store as a table. As seen earlier, an $m = 3$, $n = 6$ local model closely approximates the dynamics of our example CML ($N = 128$, $\epsilon = 0.1$). Such a model can contain at most $2^{16} = 65,536$ symbol patterns, whereas the corresponding global model could have up to $2^{128 \times 6}$.

A table of local symbol patterns can effectively replace Eq. (2) if we associate with each entry the mean CML state observed for that symbol pattern. The resulting data structure is a lookup table (LUT) mapping symbol patterns to an expected value at that site. A LUT assembled from a finite time data set may not be complete; however, we can default to LUTs of lesser symbol depths to fill in missing entries. The trade-off is that rare symbol patterns will not be resolved as well as common ones.

We find that the $m = 3$ LUT assembled from 10^5 iterations of our example CML gives an error that is almost identical to that from interval analysis for $n \leq 7$. In Fig. 2(b) we have plotted the error (triangles) of the $m = 3$, $n = 6$ LUT as a function of ϵ. For very strong coupling ($\epsilon \geq 0.25$), the LUT is *superior* to the global ($m = 128$, $n = 16$) symbolic model, in spite of the lower symbol depth. We note that the expected value produced by the LUT is weighted by the natural invariant density, which is information not used in Eq. (2). This extra information results in an improved estimate, at least for typical orbits.

The second point we wish to emphasize is that local symbolic models can be used to construct arbitrary global states and connecting orbits for the purpose of controlling spatiotemporal chaos or for transmitting information [8]. In sequence space chaos control is straightforward: we may simply append the desired target symbol sequence onto the end of the current symbolic state [9]. Mapping the modified sequence back to state space gives us the connecting orbit to the target state. In this setting the error E of the symbolic model is equivalent to the control signal amplitude needed to steer the CML along this orbit.

Take as a control example the challenge of steering a logistic CML ($\epsilon = 0.1$) along the symbolic trajectory represented by the 480×363 image [10] shown in Fig. 3 (inset). The black and white pixels are interpreted as 0 and 1 symbols, respectively, and each row as the symbolic state of a CML. That is, a CML site is greater than 0.5 only if the corresponding pixel is white. For dynamical reasons we doubled the pixel dimensions to 960×726 and replaced every black pixel with a 2×2 checkerboard of white and black pixels, thereby eliminating blocks of consecutive 0s. Using Eq. (2) we found that all the $m = 3$ local symbol patterns in this modified image are allowed by the CML dynamics for $n \leq 6$. The $N = 726$, $\epsilon = 0.1$ CML orbit corresponding to this symbol sequence is shown in Fig. 3. The first 50 iterates of Eq. (3) are uncontrolled. After iteration 50, the CML state is steered toward the orbit described by the image symbols. The target states were read from the $m = 3$, $n = 6$ LUT described earlier.

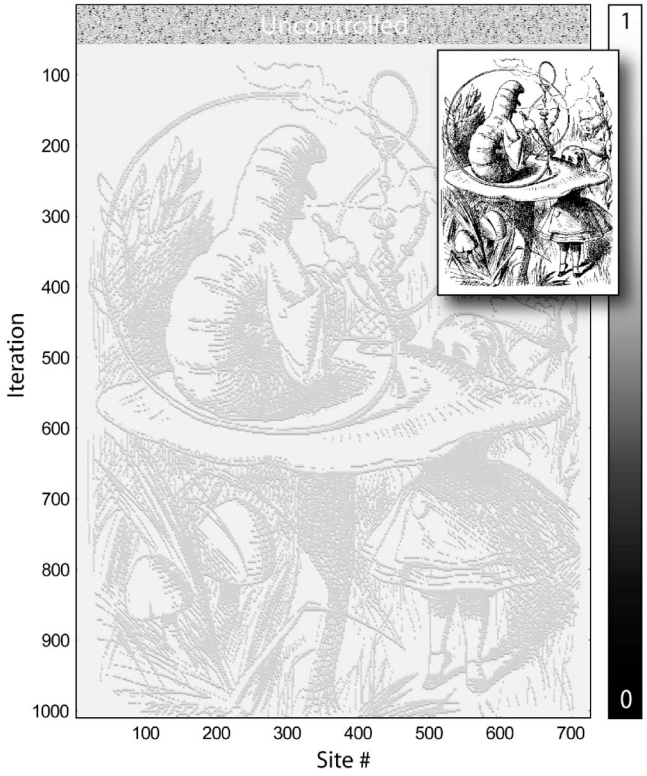

FIG. 3. A time-space plot of a 1D CML of 726 logistic maps. CML site values are displayed on a compressed gray scale $x \to [\tanh(4x - 2) + 0.964]/1.928$. Prior to iteration 50 the CML is uncontrolled. At iteration 50 a complex orbit is targeted that approximates the image shown in the overlay.

The mean perturbation required to force the CML along this orbit was found to be 0.007, which is less than 1% of the $[0, 1]$ dynamical range at each site. This assumes a controller that pushes the system state exactly onto the desired orbit at each time step. One-sided limiter control [11] produces the same results, but with slightly higher control perturbations (0.011). We conclude that local symbolic models extracted from data can be used to control spatiotemporal chaos in diffusive CMLs.

Finally, we present a closing example in the interest of broadening the applicability of the local symbolic model approach. Consider the following set of ordinary differential equations (ODEs):

$$\begin{aligned} \dot{u}_i &= 0.5 - 4v_i + \kappa(u_{i+1} + u_{i-1} - 2u_i), \\ \dot{v}_i &= -v_i + 2\max[u_i - 8\cos t - 16, 0], \end{aligned} \tag{4}$$

where $i = 1, \ldots, 1000$. This is a driven reaction-diffusion system that exhibits fully developed spatiotemporal chaos for $\kappa \in [0, 0.02]$. The solitary oscillator ($\kappa = 0$) is Rössler-like, but with regular timing. The stroboscopic return map $u_i(k\phi) \to u_i([k + 1]\phi)$, k integer, $\phi = 4.0212$, is approximately 1D and unimodal. These features suggest that $\mathbf{u}(k\phi) \to \mathbf{u}([k + 1]\phi)$, $\kappa \geq 0$, acts like a diffusive CML and can be reduced to a local symbolic model. As a test case we choose $\kappa = 0.01$ and consider 10^3 cycles of the ODE system. The resulting $10^3 \times 10^3$ data set $\{u_i(k)\}$ is symbolized by setting $s_i(k)$ to 1 where $u_i(k) > u_p$ and to 0 everywhere else. To be consistent with our CML ansatz, u_p should map to the peak of the $\kappa = 0$ return map. We estimate $u_p \approx 7.6$ by locating $\sup\{u_i(k)\}$ and taking the prior iterate at that site. From these data we construct an $m = 3$ LUT and compute $E(n)$ over a new $10^3 \times 10^3$ data set. As before, we find a smooth exponential decline of E vs n. At $n = 13$ the error is less than 1% of the dynamic range of the data. For this ODE system, the local symbolic model performs almost as well as it does for Eq. (3).

We conclude that complex systems that can be modeled as diffusively coupled lattices of unimodal maps are likely to have a compact description in terms of local symbolic models. For these systems chaos control is straightforward and novel global states can be predicted and targeted from measured data. The approach discussed here is easily generalized to multidimensional lattices of maps with more than two symbols. We think it likely that any small in-degree network of such maps is a good candidate for reduction to a local symbolic model. It remains an open question as to whether networks of invertible maps or multidimensional maps can be treated similarly.

[1] K. Kaneko, *Formation, Dynamics, and Statistics of Patterns*, edited by K. Kawasaki *et al.* (World Scientific, Singapore, 1990).
[2] B. P. Kitchens, *Symbolic Dynamics* (Springer, New York, 1998); B.-L. Hao and W.-M. Zheng, *Applied Symbolic Dynamics and Chaos* (World Scientific, Singapore, 1998).
[3] S. D. Pethel, N. J. Corron, and E. Bollt, Phys. Rev. Lett. **96**, 034105 (2006); L. A. Bunimovich and Ya. G. Sinai, Nonlinearity **1**, 491 (1988); B. Fernandez and P. Guiraud, Discrete Contin. Dyn. Syst. Ser. B **4**, 435 (2004); B. Fernandez and M. Jiang, Ergod. Theory Dyn. Syst. **24**, 107 (2004); W. Just, J. Stat. Phys. **90**, 727 (1998); **105**, 133 (2001).
[4] S. Jalan, J. Jost, and F. M. Atay, Chaos **16**, 033124 (2006).
[5] K. Kaneko, Prog. Theor. Phys. **74**, 1033 (1985).
[6] Z. Galias, Int. J. Bifurcation Chaos Appl. Sci. Eng. **11**, 2427 (2001).
[7] H. A. Yamani and M. S. Abdelmonem, J. Phys. A **30**, 2889 (1997).
[8] S. Hayes, C. Grebogi, and E. Ott, Phys. Rev. Lett. **70**, 3031 (1993); P. Garcia, A. Parravano, M. G. Cosenza, J. Jiménez, and A. Marcano, Phys. Rev. E **65**, 045201(R) (2002).
[9] N. J. Corron and S. D. Pethel, Phys. Lett. A **313**, 192 (2003); E. Bollt and E. Kostelich, Phys. Lett. A **245**, 399 (1998).
[10] L. Carroll, Alice in Wonderland, www.gutenberg.org/etext/114. Image is file alice15a.gif.
[11] N. J. Corron, S. D. Pethel, and B. A. Hopper, Phys. Rev. Lett. **84**, 3835 (2000).